Zonal Superrotation above Venus' Cloud Base Induced by the Semidiurnal Tide and the Mean Meridional Circulation*

ARTHUR Y. HOU**

Atmospheric and Environmental Research, Inc., Cambridge, Massachusetts

STEPHEN B. FELS

Geophysical Fluid Dynamics Laboratory, Princeton University, Princeton, New Jersey

RICHARD M. GOODY

Harvard University, Cambridge, Massachusetts

(Manuscript received 26 October 1989, in final form 19 February 1990)

ABSTRACT

We have calculated the equilibrium zonal wind structure resulting from the interaction of the semidiurnal tide and the mean meridional circulation driven by the zonally averaged solar heating above the Venus cloud base. The results show that the tidal mechanism proposed by Fels and Lindzen can account for a substantial fraction—and possibly all—of the increase of the equatorial wind speed above the cloud base. Above the cloud tops, tidal deceleration may be too small to produce the zonal wind decrease with height inferred from thermal data. Tidal forcing does not explain the superrotation below the clouds and additional eddy sources are needed to account for the zonal wind structure at mid and high latitudes.

1. Introduction

Fels and Lindzen (1974) first proposed that thermal tides might be responsible for the observed superrotation in the Venus clouds. In the following year, Gierasch (1975) drew attention to the importance of momentum transport by the meridional (Hadley) circulation. Both of these phenomena may be investigated numerically, given certain parameters of the Venus atmosphere, most of which are available from the Pioneer Venus and Venera missions.

The idea that the superrotation might be a direct result of equilibration between these two effects must have been in the minds of many investigators, although it appears to have been first explicitly proposed by Hou (1984) and Hou and Goody (1985). Although the calculations of Venus tides by Pechmann and Ingersoll (1984) did not at first appear to support this idea, later studies by Valdes (1985) and Fels (1986) showed that the Eliassen–Palm (EP) flux convergence due to the semidiurnal tide may be of the same order of magnitude as that required for maintaining the cloud top circulation, as diagnosed by Hou and Goody. If the observed winds are indeed a result of the equilibrated tidal forcing with the mean flow, it would constitute a direct explanation of this intriguing problem; it is important to demonstrate this quantitatively.

An attempt to do so was made by Baker and Leovy (1987). They adapted a terrestrial model of the zonal mean circulation and the semidiurnal tide to Venus conditions, and integrated it forward for 50 days from an initial state of superrotation similar to that observed. They showed that the tide and the mean flow adjust rapidly away from the tropics to achieve equilibration with the zonal wind at the equator; but the equatorial wind itself did not equilibrate in 50 days (we shall later show that approximately 10 times this period is required). In a companion paper, Leovy (1987) used a simple heuristic model to show that the balance between tidal forcing and the Hadley circulation could, for certain parameter ranges, reproduce the observed superrotation at the equator. The two results, taken together, appear to give a positive but equivocal answer to our question.

* This paper, completed shortly after Steve Fels' death, is an appropriate memorial to one important phase of a productive scientific career. Fels and Lindzen (1974) first raised the possibility that the Venus superrotation might be driven by tides, and Steve returned to this problem on a number of occasions. He would have been pleased with our limited results, had he lived to see them.

Richard Goody, Arthur Hou

** Present affiliation: Laboratory for Atmospheres, NASA/Goddard Space Flight Center.

Corresponding author address: Dr. Arthur Y. Hou, Laboratory for Atmospheres, Code 911, NASA/GSFC, Greenbelt, MD 20771.

In this paper, we present equilibrated solutions for the mean circulation and the semidiurnal tide. Despite time and cost limitations, which prevented us from exploring the full range of poorly determined atmospheric parameters, our results are sufficient to show that the observations can be at least partly explained by these two processes.

2. The model

Studies of the Venus tides by Pechmann and Ingersoll (1984) and Valdes (1985) showed that the vertical wavelength of the diurnal tide is much shorter than the depth of the heating region; destructive interferences of waves excited at different levels make it unlikely that the diurnal tide can be effective in forcing the entire heating region. We will, therefore, consider only the semidiurnal tide in this investigation.

Calculations of the semidiurnal tide (op. cit.) showed that it requires a vertical resolution of one gridpoint per kilometer to resolve the tides, making an interactive 2-D tidal and mean circulation model an expensive proposition. An alternative is to couple a high resolution tidal model with a zonally averaged circulation model. Fels and his collaborator (Fels et al. 1984, Fels 1986) developed an efficient, high resolution, WKBJ model of Venus' semidiurnal tide and showed it to be in good agreement with observations and also with the calculations by Valdes (1985) using a sophisticated tidal model.

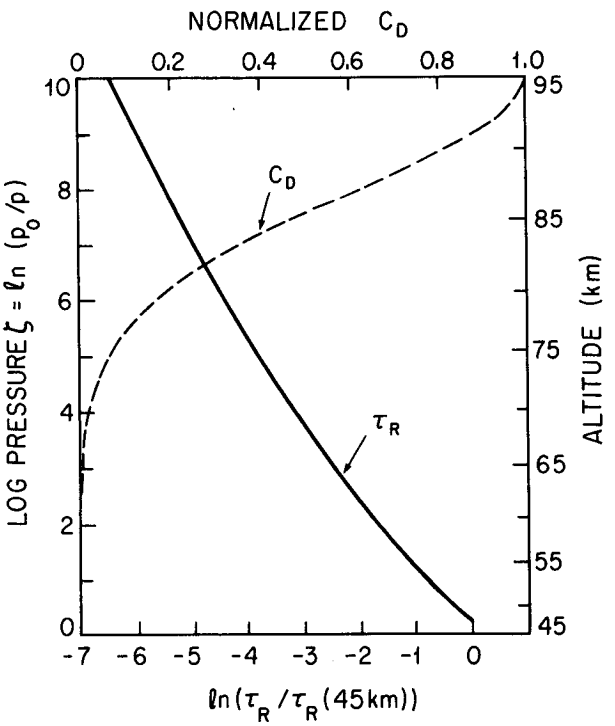

FIG. 2. The radiative relaxation time, τ_R, for the mean temperature [scaled by τ_R (45 km) = 10^7 s] and the Rayleigh friction coefficient, C_D, scaled by C_D (95 km) = 0.2 d^{-1} (in the standard case).

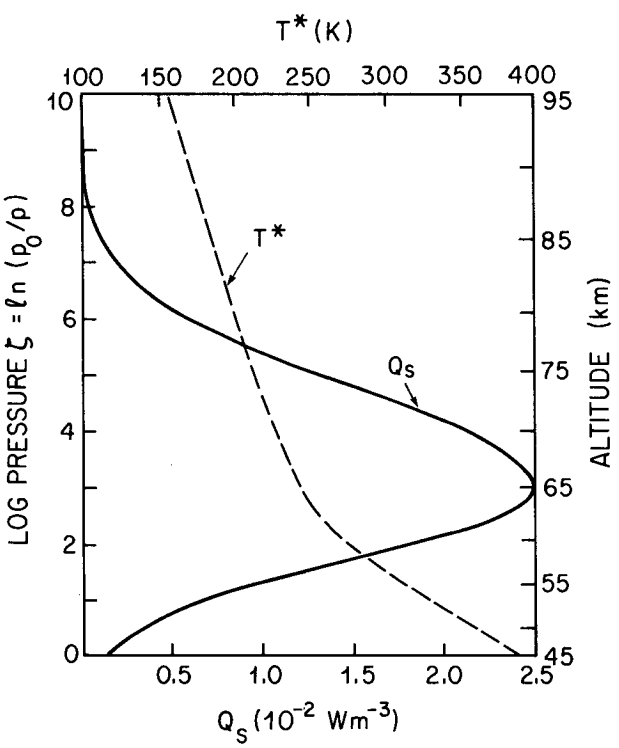

FIG. 1. The solar heating for an overhead sun, Q_S, from Hou and Goody (1989) and the latitudinal mean temperature, T^*, from Fels (1986).

We have incorporated Fels' tidal model into the zonally averaged primitive equation model of Hou and Goody (1985) and calculated the steady zonal-mean circulation and temperatures resulting from the mean solar heating and the semidiurnal tide. Since the flow in the deep interior is probably maintained by processes other than tidal (see Hou and Farrell 1987; Hou and Goody 1989), we shall prescribe the zonal wind at the cloud base (~45 km) and investigate the effect of tidal forcing above this level. At each time step, the tidal subroutine computes the semidiurnal EP flux divergence for the instantaneous zonal mean structure, and the zonal mean model calculates the circulation and temperatures forced by the tide and the mean solar drive.

Unless noted otherwise, the parameters for the tidal model are those of Fels et al. (1984) and Fels (1986). The zonal mean circulation model is that of Hou and Goody (1985), except for the following: the model extends from the cloud base at 45 km (p_o = 2 bars) to 95 km [$p \approx p_o \exp(-10)$], where p is pressure and p_o the pressure at the lower boundary. It employs the solar heating model of Hou and Goody (1989) and a latitudinal mean temperature consistent with Fels' tidal model (see Fig. 1). The radiative relaxation times for the mean temperatures are shown in Fig. 2 and are comparable to the values used by Baker and Leovy.

The scale-dependent radiative relaxation times for the semidiurnal tide are those used by Fels et al. (1984) (i.e. twice the values in Fig. 2, with an upperbound of 10^7 s). The ad hoc diffusion term is omitted in the heat equation and the zonal wind at the lower boundary is relaxed to solid body rotation with an equatorial wind speed of 50 m s^{-1}. Near the upper boundary we used a Rayleigh drag (relaxing to the same profile as the zonal wind at the lower boundary); we shall show that this does not affect the results below the drag layer. The drag coefficients are shown in Fig. 2. In the control runs, the momentum damping rate is 0.2 d^{-1} at 95 km and the damping rates below 85 km are more than an order of magnitude smaller than those used by Baker and Leovy. To ensure computational stability, the model employs a small vertical diffusion of momentum, with a coefficient of $\nu = 2.5$ m^2 s^{-1}, consistent with upperbound estimates from chemical measurements by von Zahn et al. (1983). For a higher vertical resolution, it could be even smaller.

3. Results

In order to isolate the effect of the semidiurnal tide, we performed calculations with and without the tide.

a. Without tidal forcing

Figure 3 shows that the mass streamfunction for the meridional circulation forced by the zonal mean solar heating corresponds to a thermally direct cell centered

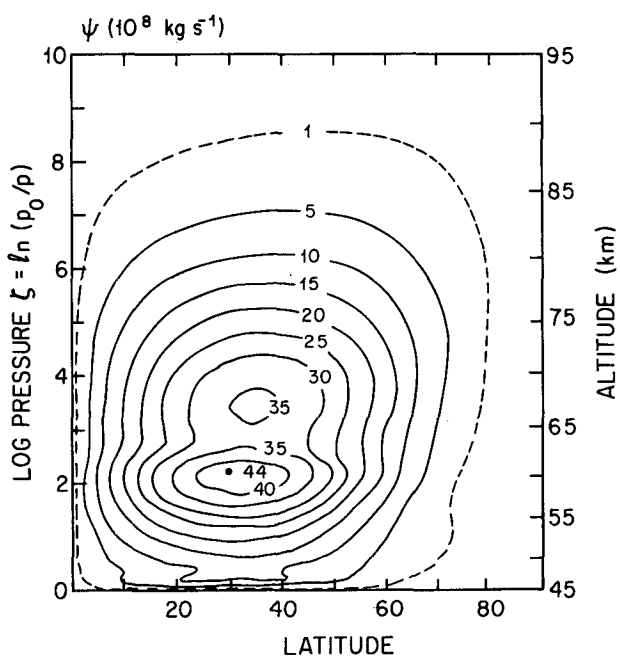

FIG. 3. The meridional mass streamfunction for the residual circulation forced by the zonally averaged solar heating in the absence of the semidiurnal tide.

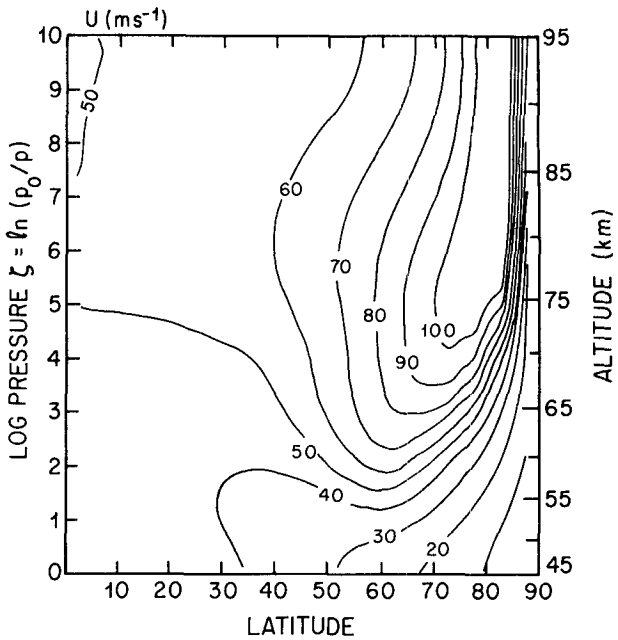

FIG. 4. Zonal winds in the absence of the semidiurnal tide.

near the level of maximum heating. Figure 4 shows the computed zonal winds. At the equator the wind speed is 50 m s^{-1} at all levels, in agreement with Hide's theorem, which requires that the equatorial atmosphere does not superrotate in the absence of up-gradient transport of absolute angular momentum. This is qualitatively different from the observed equatorial zonal wind, which increases with altitude by about a factor of 2 between 45 and 70 km and, according to interpretations of Venus thermal data (Schubert 1983), decreases with height above 70 km to close to zero at 100 km.

Figure 5 shows the observed and calculated zonal winds at the cloud tops, ($\approx$70 km). As a result of transport by the Hadley cell, the zonal wind increases with latitude and terminates with a jet near the pole, as predicted by the simple model of Hou (1984) for a slowly rotating atmosphere; the winds resemble the angular-momentum-conserving profile [Eq. (12) of Hou] for an equatorial wind speed of 50 m s^{-1}. The strength and the latitude of the calculated zonal jet depends to some extent on the dissipation in the model; but its poleward location relative to the observed jet is consistent with the prediction that a slower equatorial circulation has a more poleward jet.

Figure 6 shows the calculated temperatures. They are close to thermal wind balance with the zonal wind and show little variations with latitude, except at high latitudes, where zonal winds have large vertical shears. Above 75 km, the slight increase of temperature with latitude equatorward of the jet is a result of the small negative vertical wind shear induced by the Rayleigh drag near the upper boundary.

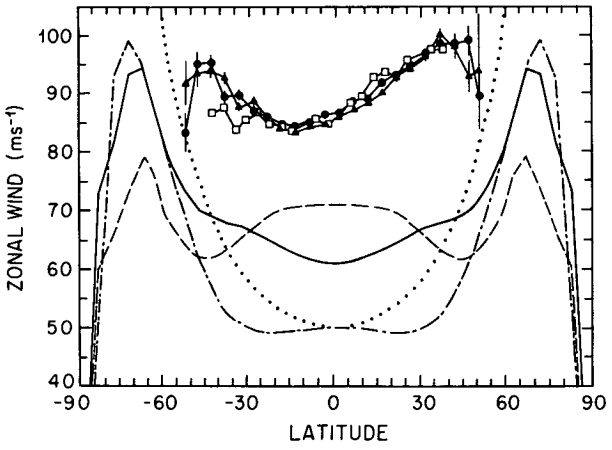

FIG. 5. Observed and model zonal winds at 70 km for (i) no tide (long-short dashes), (ii) with tide (full line), (iii) reduced mean solar heating (broken line), (iv) the angular momentum conserving profile [dots, from Hou 1984, Eq. (12)], and (v) observations [squares are from Rossow (1985), circles and triangles correspond to Data Sets A and B from Limaye et al. (1988)].

b. *With tidal forcing*

With tidal forcing included in the calculation, we integrated the model forward until the tendency terms were at least two orders of magnitude smaller than the leading terms in the prognostic equations. Typically, this required 600 to 700 Earth days. The initial state for all calculations was solid body rotation with an equatorial speed of 50 m s^{-1}.

The equilibrated zonal wind field is shown in Fig. 7. Figure 5 compares the zonal wind at the cloud tops to the observations and to the case of no tidal driving. Similarly, Fig. 8 compares the vertical profiles of the zonal wind at the equator. The results show that tidal forcing leads to a maximum equatorial zonal wind of slightly greater than 60 m s^{-1} (an increase of 10 m s^{-1} over the background rotation) at the cloud tops; the winds decrease with distance above and below this level, consistent with tidal mechanism proposed by Fels and Lindzen (1974). Above 80 km, the winds are influenced by the drag (see section 3c). Figure 5 shows that the zonal winds are affected by the tide mostly in the tropics. At the high latitudes, tidal effects are small and the zonal wind structure is determined primarily by the mean circulation.

We do not show the *residual* meridional streamfunction since it differs little from Fig. 3, except that the maximum is 10% weaker, consistent with the increased atmospheric rotation rate (see Hou 1984). The calculated poleward residual velocities are 2–3 m s^{-1} in the 75 to 80 km region and the return flow reaches a maximum of about −0.2 m s^{-1} just below 65 km. Similarly, the temperature field deviates only slightly from Fig. 6.

Despite a certain qualitative resemblance between the model results and observations, the computed maximum zonal wind induced by the mean solar heating and the semidiurnal tide is considerably weaker than is observed. Hou and Goody (1985; 1989) have calculated the net mean flow forcing (i.e. $G + F$ in their notation) required for maintaining the observed circulation. It is instructive to compare the tidal EP flux divergence in the present study with this require-

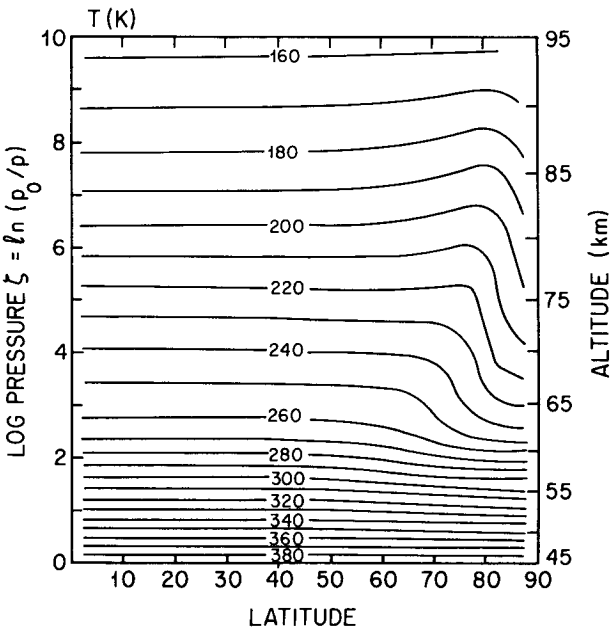

FIG. 6. Temperatures in the absence of the semidiurnal tide.

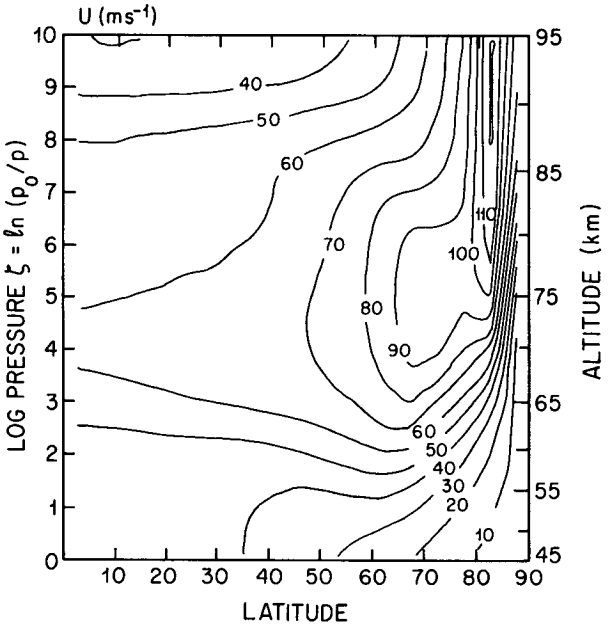

FIG. 7. Equilibrated zonal wind in the presence of the semidiurnal tide.

ment and with those obtained by Fels (1986) and Valdes (1985) using the observed zonal winds.

Figures 9 and 10 show the tidal acceleration in m s^{-2} and the density weighted EP flux divergence from the present calculation. Below 85 km, these results correspond quite well with those of Fels and Valdes, even though the calculations involved different zonal winds. Our maximum equatorial zonal wind is about half of those used by Fels and Valdes; yet our maximum equatorial acceleration of 0.38 m s^{-1} d^{-1} compares closely with 0.3 m s^{-1} d^{-1} of Fels and is about 3 times that of Valdes. At 80 km, our deceleration is half those of both Fels and Valdes and our maximum deceleration at 90 km is half that of Valdes but slightly larger than that of Fels. An obvious qualitative difference is that the region of acceleration at 85 km (with a maximum near 60° latitude) extends to the equator in our case but not in Fels' and Valdes'. This may be due to the rapid variation of zonal wind near 85 km, which may invalidate the WKBJ approximation locally. It will be shown in section 3c that our results above 80 km are influenced by the upper boundary drag; but, below 80 km, our results are in substantial agreement with those of Fels and Valdes, both in terms of the overall structure and magnitude.

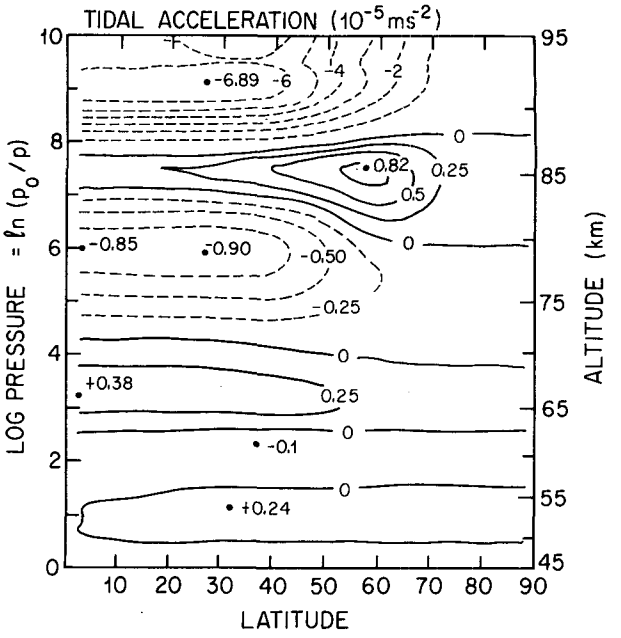

FIG. 9. Mean flow acceleration due to the semidiurnal tide.

We can compare the tidal EP flux divergence in Fig. 10 with the net mean flow forcing needed for maintaining the observed circulation calculated by Hou and Goody (1989, Fig. 9a), which is reproduced in Fig. 11. It is clear that the required eddy sources and sinks in the middle and high latitudes simply cannot be satisfied by the semidiurnal tide, nor can they be explained by the diffusion in the model (which is down-gradient). As discussed in Hou (1984), these midlatitude source requirements are induced by horizontal motions across the zonal jet, where the angular momentum changes abruptly, and must therefore be signatures of local eddy processes which help shape the observed jet. The jet in the present calculation is controlled by the mean cir-

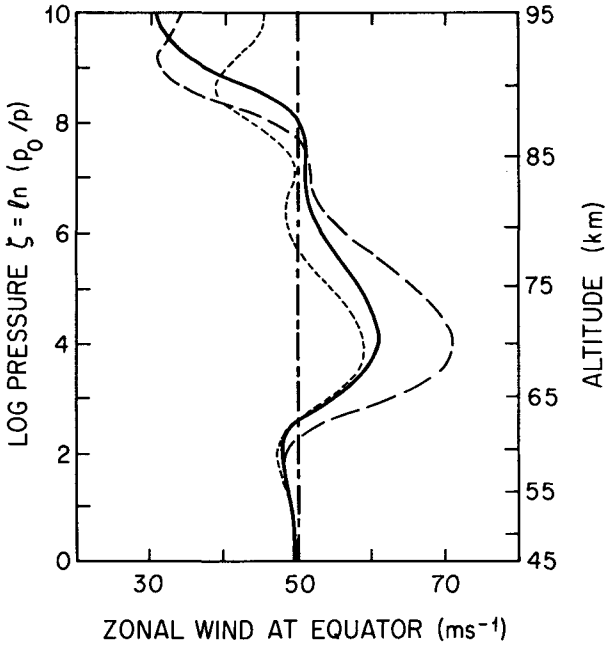

FIG. 8. Equatorial zonal winds. The key is the same as for Fig. 5. The short dashes are for the case of increased upper level drag.

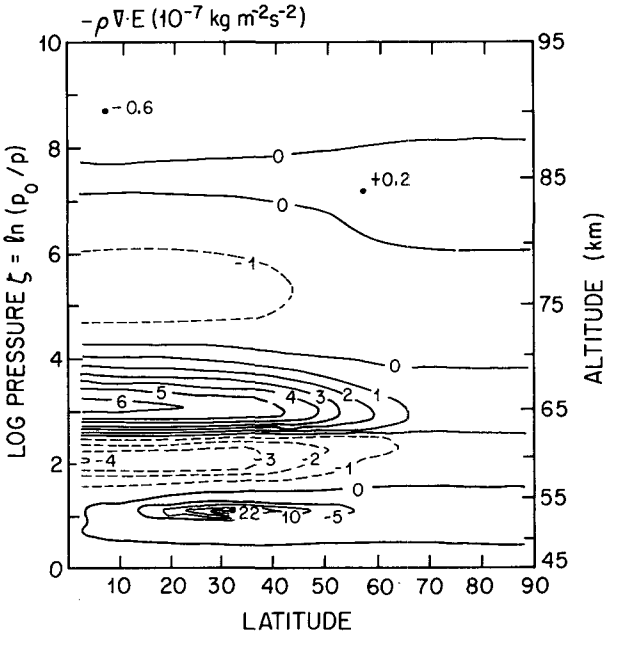

FIG. 10. Density-weighted Eliassen–Palm flux divergence for the semidiurnal tide.

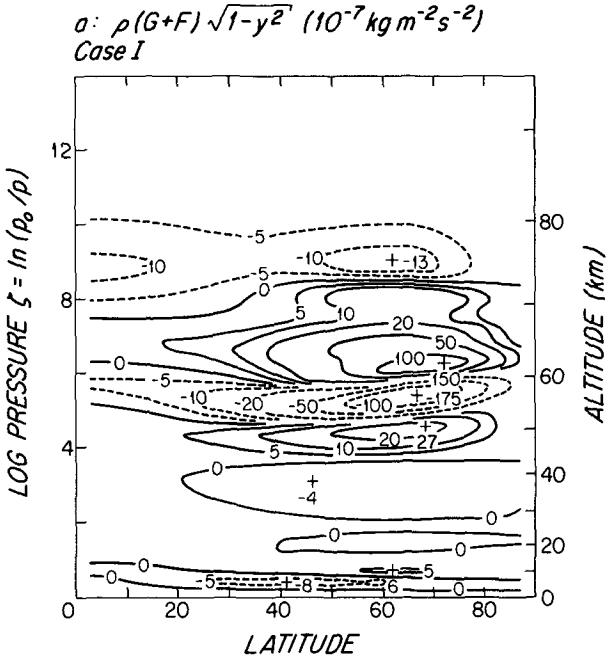

FIG. 11. The net mean flow forcing required for maintaining the observed zonal wind on Venus [reproduced from Fig. 9a of Hou and Goody (1989)]. This result is for a zonal wind with a midlatitude jet (their Case I, see Hou and Goody for details). Note that their reference pressure, p_o, is 90 bars.

culation and diffusion, and differs from the observations (see Fig. 5), which also argues for the presence of midlatitude eddy sources. However, if the influence of these sources on the mean flow is restricted to mid and high latitudes, they are probably not central to the problem of equatorial superrotation.

Figure 12 shows that, at the equator, the tidal EP flux divergence at 65 km is slightly larger than the required mean flow forcing determined by Hou and Goody (1989, Fig. 10, Case I); but in the present calculation, nearly a half of the tidal acceleration at 65 km is offset by diffusive losses, leading to a weaker net forcing and a smaller maximum wind speed than is observed. The precise value of mixing coefficient is, of course, not known and there could be large spatial variations, as in the earth's stratosphere (Newman et al. 1988). A smaller mixing coefficient in the tropics (as in the case of Earth's stratosphere) would probably bring the maximum wind speed closer to the observed (see section 3). Above 70 km, tidal decelerations are too small to account for the observed zonal wind decrease above the cloud tops. However, there are no direct wind measurements in this region and one cannot rule out the possibility that inferences from thermal data are in error.

c. *Sensitivity tests*

The long term structure of the Venus atmosphere is not known with any degree of certainty; we have, therefore, tested our results for sensitivity to plausible variations in model parameters. We pay special attention to processes that control the zonal wind at the equator, which we believe to be the key issue in the superrotation problem.

At the equator, the equilibrated zonal wind is determined by a balance between tidal acceleration, vertical advection by the Hadley circulation, and friction. In the results presented in the previous section, at the cloud tops, advection by the Hadley cell offsets about 60% of the tidal forcing, while diffusion balances the remaining 40%. This may appear to contradict our earlier studies (Hou and Goody 1989), which showed that—in terms of latitudinal averages—the cloud top circulation is essentially inviscid. What we find here is that, near the equator, the advective terms are smaller and diffusion is comparatively more important. Since the value of the mixing coefficient at the equator is uncertain, we reduced the mixing coefficient from 2.5 to 1.0 $m^2 s^{-1}$ to see if a lower value of diffusion could increase the equatorial wind speed; but this led to numerical instabilities at the current model resolution. Instead, we performed an experiment in which the mean solar heating was reduced by 25%, while the tidal heating remained the same. This serves as a test of the effect of varying the ratio of tidal pumping to Hadley transport. Figures 5 and 8 show that, at the equator, the maximum zonal wind at the cloud top increases to 70 m s^{-1} (i.e. the speed increment is doubled) and that the latitude of the jet decreases. While these two features show an improved relation to the observations,

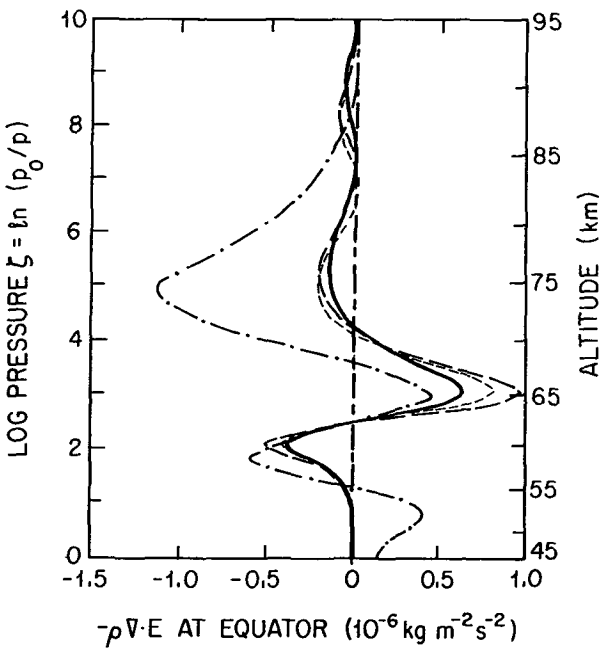

FIG. 12. Density weighted EP flux divergence at the equator. The key is the same as for Fig. 5. Also shown is the equatorial source requirement (dash-dots) from Hou and Goody (1989).

the winds in the midlatitudes are less satisfactory, which may be interpreted as yet another indication of missing eddy sources in this region (see section 3b).

Curiously, here as in all other examples, tidal forcing causes the same increase of wind speed between 45 and 70 km as the decrease from 70 to 85 km. This is also true for the transient adjustment during an initial spin-up, as can be seen in Fig. 13a of Baker and Leovy (1987).

Leovy (1987) showed that the feedback between the tide and the mean flow may be positive or negative, depending on model parameters. Figures 8 and 12 show that tidal forcing at the maximum heating level ($\sim$65 km) increases with the strength of the equatorial jet, suggesting a positive feedback for the adopted model parameters. Such a positive feedback would lead to instability, as pointed out by Leovy—unless, of course, diffusion is present to act as an additional restoring force, as in these calculations.

Figures 8 and 12 also show that in response to increased tidal forcing at 65 km, the zonal wind develops a stronger vertical shear near the jet, resulting in increased diffusive losses to partially offset the increased tidal pumping. Our experience with 2-D models suggests that by increasing the vertical resolution, it may be possible to obtain a still larger equatorial jet for a smaller value of ν.

The radiative relaxation times for the semidiurnal tide used by Baker and Leovy (1987) were those of Crisp (1983), which were for a cloudy atmosphere; at 65 km, these values are about half of those used by Fels (1984) for a pure CO_2 atmosphere. We performed a calculation using half of the radiative damping times shown in Fig. 2, and found little difference.

We tested the influence of the upper level drag by increasing the damping rate at 95 km from 0.2 to 0.5 d^{-1}. Figure 8 shows that the zonal wind reflects the influence of this upper-level drag (which relaxes the wind to the background speed of 50 m s^{-1}) above 80 km, but that the effect is small below this level.

4. Conclusions

This work has been an attempt to evaluate the effects of the semidiurnal tide and the Hadley circulation and their contributions to the Venus superrotation. Although our treatment is incomplete in some respects, the results are sufficient for us to conclude that these two processes may account for a substantial part of the observed superrotation above the cloud base. At the equator, tidal forcing produces a maximum zonal wind speed at the same level as the observed maximum, but may be insufficient to explain the total velocity increment between the cloud base (45 km) and the maximum level (65 km). Our calculations show an increment 2 to 3 times too small, although uncertainties in the data are such that results much closer to observations might be obtained with other plausible parameters.

Our results show that even if good agreement could be achieved with the incremental speed above the cloud base, major discrepancies remain between tidal forcing and the eddy source requirements calculated by Hou and Goody. Since the tidal response is confined to regions above the observed static stability minimum near 55 km (see Valdes 1985), tidal forcing could not account for the speed of 50 m s^{-1} at 45 km, which is prescribed in our calculations. Also, tidal deceleration above the clouds appears to be too small to explain the observed wind decrease above 70 km. It is possible that other mechanisms such as breaking gravity waves may decelerate the mean flow at these heights, as they do in Earth's mesosphere.

Away from the equator, the tidal EP flux divergences in middle and high latitudes cannot satisfy, either qualitatively and quantitatively, the eddy source requirements of Hou and Goody. Again, this result might be modified given better zonal wind data; but given our present knowledge, there appears to be a discrepancy, suggesting the presence of other eddy processes at these latitudes.

Tidal drives are demonstrably important but they are only one of the wave-mean-flow interactions required to explain the circulation of the Venus atmosphere. To reconcile the many discrepancies between the tidal results and observations, there are a variety of other eddy mechanisms to consider (see Rossow 1985, for a review), including Rossby and Kelvin waves (Belton et al. 1970; Covey and Schubert 1982; Del Genio and Rossow 1989), critical layer absorption of gravity waves (Hou and Farrell 1987), baroclinic instability (Young et al. 1984), barotropic instability (Rossow 1983; Elson 1989), and topographic waves (Gierasch 1988). Unlike the tides, however, these eddy processes are far more difficult to quantify; much work will be needed before a more complete description of the Venus circulation is possible.

Acknowledgments. This work was supported by the NASA Planetary Atmosphere Program under Contract NASW-4206 to AER and NGL-22-007-228 to Harvard University. The computations were performed at the NSF John von Neumann National Super Computing Center.

REFERENCES

Belton, M. J. S., G. R. Smith, G. Schubert and A. D. Del Genio, 1976: Cloud patterns, waves and convection in the Venus atmosphere. *J. Atmos. Sci.*, **33**, 1394–1417.

Baker, N. L., and C. B. Leovy, 1987: Zonal winds near Venus' cloud top level: A model study of the interaction between the zonal mean circulation and the semidiurnal tide. *Icarus*, **69**, 202–220.

Covey, C., and G. Schubert, 1982: Planetary-scale waves in the Venus atmosphere. *J. Atmos. Sci.*, **39**, 2397–2413.

Crisp, D., 1983: *Radiative Forcing of the Venus Mesosphere.* Ph.D. thesis, Princeton University, 193 pp.

Del Genio, A. D., and W. B. Rossow, 1989: Planetary scale waves and the cyclic nature of cloud top dynamics on Venus, submitted to *J. Atmos. Sci.*

Elson, L. S., 1989: Three-dimensional linear instability modeling of cloud level Venus atmosphere. *J. Atmos. Sci.*, **46**, 3559–3568.

Fels, S. B., 1986: An approximate analytical method for calculating tides in the atmosphere of Venus. *J. Atmos. Sci.*, **43**, 2757–2772.

——, and R. S. Lindzen, 1974: The interaction of thermally excited gravity waves with mean flows. *Geophys. Fluid Dyn.*, **6**, 149–192.

——, J. T. Schofield and D. Crisp, 1984: Observations and theory of the solar semidiurnal tide in the mesosphere of Venus. *Nature*, **312**, 431–434.

Gierasch, P. J., 1975: Meridional circulation and the maintenance of the Venus atmospheric rotation. *J. Atmos. Sci.*, **32**, 1038–1044.

——, 1988: Waves in the atmosphere of Venus. *Nature*, **328**, 510–512.

Hou, A. Y., 1984: Axisymmetric circulations forced by heat and momentum sources: A simple model applicable to the Venus atmosphere. *J. Atmos. Sci.*, **41**, 3437–3455.

——, and R. M. Goody, 1985: Diagnostic requirements for the superrotation on Venus. *J. Atmos. Sci.*, **42**, 413–432.

——, and B. F. Farrell, 1987: Superrotation induced by critical-level absorption of gravity waves on Venus. *J. Atmos. Sci.*, **44**, 1049–1061.

——, and R. M. Goody, 1989: Further studies of the circulation of the Venus atmosphere. *J. Atmos. Sci.*, **46**, 991–1001.

Leovy, C. B., 1987: Zonal winds near Venus' cloud top level: An analytic model of the equatorial wind speed. *Icarus*, **69**, 193–201.

Limaye, S. S., C. Grassotti and M. J. Kuetemeyer, 1988: Venus: Cloud level circulation during 1982 as determined from Pioneer cloud photopolarimeter images. Part 1: Time and zonally averaged circulation. *Icarus*, **73**, 193–211.

Newman, P. A., M. R. Schoeberl and R. A. Plumb, 1986: Horizontal mixing coefficients for two-dimensional chemical models calculated from National Meteorological Center data. *J. Geophys. Res.*, **91**, 7919–7924.

Pechmann, J., and A. P. Ingersoll, 1985: Thermal tides in the atmosphere of Venus: Comparison of model results and observations. *J. Atmos. Sci.*, **41**, 3290–3313.

Rossow, W. B., 1983: A general circulation model of a Venus-like atmosphere. *J. Atmos. Sci.*, **40**, 273–302.

——, 1985: Atmospheric circulation of Venus. *Advances in Geophys*, Vol. 28A, S. Manabe, Ed., Academic Press, 581 pp.

Valdes, P. J., 1985: Large Scale Waves in the Atmosphere of Venus. Ph.D thesis, Oxford University, 400 pp.

von Zahn, U., S. Kumar, H. Niemann and A. Kliore, 1985: Composition of the Venus atmosphere. *Venus*, D. M. Hunten et al., Eds., University of Arizona Press, 299–430.

Young, R. E., H. Houben and L. Pfister, 1984: Baroclinic instability in the Venus atmosphere. *J. Atmos. Sci.*, **41**, 2310–2333.